ELSEVIER

Ceramics International 30 (2004) 285–290

CERAMICS INTERNATIONAL

www.elsevier.com/locate/ceramint

Photoluminescence of $4SrO{\cdot}7Al_2O_3$ ceramics sintered with the aid of B_2O_3

C.K. Chang[a,*], L. Jiang[a], D.L. Mao[a], C.L. Feng[b]

[a]*School of Materials Science and Engineering, Shanghai Jiaotong University, 1954 Huashan Road, Shanghai 200030, PR China*
[b]*Shanghai Institute of Organic Chemistry, 354 Fengling Road, Shanghai 200032, PR China*

Received 4 March 2003; received in revised form 24 March 2003; accepted 2 May 2003

Abstract

$4SrO{\cdot}7Al_2O_3$ long persistent ceramics with different B_2O_3 contents prepared by sintering were characterized by X-ray diffraction (XRD), transmission electron microscopy (TEM) and photoluminescence spectrum (PLS). The ceramics showed a two peak emission at 400 and 486 nm, due to the different lattice sites Eu^{2+} ions held in the $4SrO{\cdot}7Al_2O_3$ lattice. B_2O_3 plays several different roles in the ceramics. In the synthesis process, it greatly promotes the formation of $4SrO{\cdot}7Al_2O_3$ phosphor and helps to form dense ceramics at 1400 °C. Furthermore, with the addition of B_2O_3, the emission peaks shifted to the short wavelength side due to lattice contraction. The afterglow characteristics result from the emission at 486 nm other than the emission at 400 nm. The duration of the phosphor was enhanced by the addition of B_2O_3, due to the trap center formed in the $4SrO{\cdot}7Al_2O_3$ host.

Keywords: A. Sintering; B. X-ray methods; C. Optical properties; Luminescence

1. Introduction

Long persistent phosphors are kinds of energy-storing materials. The materials can absorb visible and UV lights, store the photon energy, and gradually release the energy as visible light that leads to a long persistent afterglow in the darkness. Recently, double oxides containing strontium and aluminum have become of interest in material science since they show excellent properties such as high quantum efficiency [1], long persistence of phosphorescence and good stability [2,3] when compared with classical sulfide phosphorescent phosphors. Based on these properties, some strontium aluminates have been employed in many fields [4].

Among the compounds in $MO–Al_2O_3$ binary system, the tridymite type aluminates activated by Eu^{2+} with long afterglow, such as $SrO{\cdot}Al_2O_3{:}Eu^{2+}Dy^{3+}$, $BaO{\cdot}Al_2O_3{:}Eu^{2+}Dy^{3+}$ and $CaO{\cdot}Al_2O_3{:}Eu^{2+}Nd^{3+}$, were well recorded in documents [5–7]. The previous studies described the synthesis method, photolwninescent property, afterglow characteristics and the long lasting mechanism of the mentioned above long lasting phosphors. It was commonly agreed that the luminescence originates from the transitions between the $^8S_{7/2}$ ($4f^7$) ground state of Eu^{2+} and the $4f^65d^1$ excited state, and that the matrix can have important influence on the luminescent properties. These findings give us hints that, new long persistent phosphors holding different emitting wavelengths will be achieved when alternating the crystal structures of the aluminate matrix. Recently, some works have been done with $4SrO{\cdot}7Al_2O_3$ as the new matrix other than the monoclinic aluminates [8,9]. However, the photoluminescent behavior of Eu^{2+} in the newly employed matrix, say $4SrO{\cdot}7Al_2O_3$, need a more intensive study.

In this study, long persistent $4SrO{\cdot}7Al_2O_3$ ceramics with different B_2O_3 contents were prepared by sintering method. The effect of B_2O_3 on both the sintering process and the luminescent properties were investigated.

2. Experimental procedure

$4SrO{\cdot}7Al_2O_3$ long persistent ceramics were obtained by high temperature sintering. Ceramics with four different B_2O_3 contents listed in Table 1 were prepared in the experiment. According to their chemical composi-

* Corresponding author: Fax: +86-21-6293-2522.
E-mail address: ckchang@mail.sjtu.edu.cn (C.K. Chang).

0272-8842/03/$30.00
doi:10.1016/S0272-8842(03)00101-9

tions, certain amounts of $SrCO_3$, α-Al_2O_3, Eu_2O_3 (99.99%), Dy_2O_3 (99.99%) and H_3BO_3 were mixed in a high speed ball mill for 4 h, and then calcified at 1300 °C for 8 h in a reducing atmosphere to form phosphors. The synthesized $4SrO{\cdot}7Al_2O_3$ phosphors were powdered again to achieve a smaller particle size and were pressed into $\phi 25\times 5$ mm tablets under pressure of 50 MPa. These tablets were then isostatically pressed under 400MPa for 5 min. The final samples were sintered at 1400 °C in a reducing atmosphere to form luminescent ceramics.

Phase identification of sintered ceramics was performed using the X-ray diffraction method. The experiments were conducted on a Rigaku D/max-3B X-ray diffractometer, using CuK_α X-rays of wavelength 1.5405 Å. The microstructures of obtained ceramics were observed using transmission electron microscope (TEM).

The excitation and emission spectrum of the sintered $4SrO{\cdot}7Al_2O_3$ ceramics were obtained by a fluorescent spectrometer (LS5OB). The decay profiles were also generated using the same instrument after the samples were sufficiently excited under UV lights. Simulating of the long persistent property was conducted employing the non-linear fitting function provided by Microcal Origin6.0 software.

Table 1
Chemical composition of sintered $4SrO{\cdot}7Al_{2-x}B_xO_3$: $Eu^{2+}Dy^{3+}$ luminescent ceramics

Nominal composition	Components (%)				
	$SrCO_3$	Al_2O_3	Eu_2O_3	Dy_2O_3	H_3BO_3
$4SrO{\cdot}7Al_{2-x}B_xO_3:Eu^{2+}Dy^{3+}$					
$x=0$	43.788	52.954	1.044	2.2 13	0
$x=0.05$	43.665	51.487	1.041	2.207	1.56
$x=0.1$	43.544	50.027	1.038	2.201	3.191
$x=0.2$	43.302	47.131	1.032	2.188	6.346

3. Results and discussion

3.1. Phase composition of $4SrO{\cdot}7Al_2O_3$ ceramics and the role of B_2O_3 in sintering process

Fig. 1a and b show the XRD patterns of $4SrO{\cdot}7Al_{2-x}B_xO_3:Eu^{2+}Dy^{3+}$ ceramics with different B_2O_3 content ($x=0$ and 0.2) sintered at 1400 °C. It can be seen from the XRD patterns that, $4SrO{\cdot}7Al_2O_3$ was formed as the main phase when sintering at temperature of 1400 °C. The obtained two ceramics show orthorhombic structure of $4SrO{\cdot}7Al_2O_3$ which is in good agreement with the results from the others [10]. The ceramics aided by B_2O_3 reveals a single orthorhombic $4SrO{\cdot}7Al_2O_3$ structure, and no other phases are identified. However, some other lines, which were not indexed as the peaks of $4SrO{\cdot}7Al_2O_3$ phase, appear in the XRD spectrum of the ceramics without B_2O_3 addition, indicating the existence of a second phase. This second phase, as marked in Fig. 1b, was confirmed to be the un-reacted Al_2O_3 introduced by the starting α-Al_2O_3.

TEM observations of the obtained ceramics are shown in Fig. 2. The grain sizes of the two ceramics are similar, about 0.5–1 μm in the observed area. It can be seen from the micrograph (Fig. 2a) that B_2O_3 aided ceramics is fully densified at 1400 °C. However, micropores, denoted as P in Fig. 2b, are observed in the microstructure of the ceramics without B_2O_3 addition. Combining these findings with XRD results, the roles of B_2O_3 in the synthesis of phosphors and the ceramic sintering process are obvious. The introduction of B_2O_3 can form liquid phase at a relatively low temperature. This liquid phase can greatly promote the formation of the long lasting phosphor and reduce the sintering temperature to obtain dense ceramics. With the help of B_2O_3, single phase $4SrO{\cdot}7Al_2O_3$ ceramics was obtained at 1400 °C, while higher temperature is required in the case of ceramics without B_2O_3 addition. Furthermore, TEM observations indicate another important role of

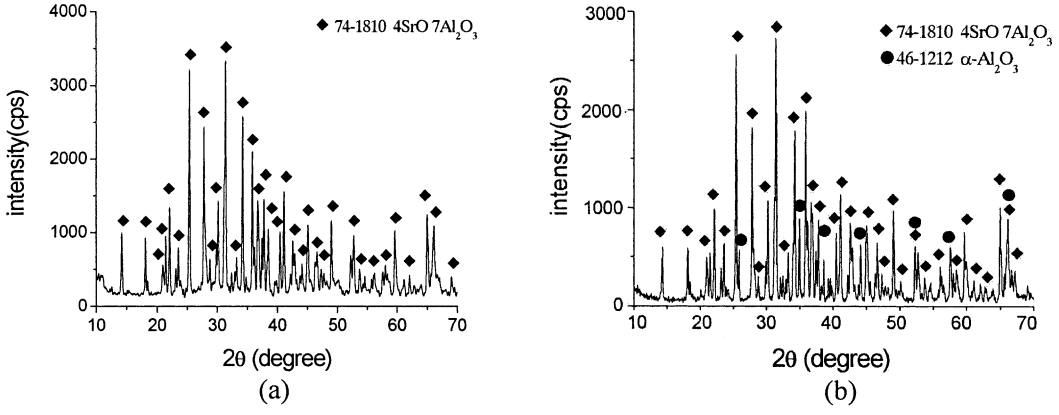

Fig. 1. XRD pattern of $4SrO{\cdot}7Al_{2-x}B_xO_3:Eu^{2+}Dy^{2+}$ ceramics (a), $x=0.2$ and (b) $x=0$.

B_2O_3 of removing the micropores on the grain boundary in the sintering process.

3.2. Excitation and emission of sintered $4SrO{\cdot}7Al_2O_3$ ceramics

Typical photoluminescent curves of $4SrO{\cdot}7Al_2O_3$ activated with Eu^{2+} are shown in Fig. 3. Curve 1 is the excitation spectrum of $4SrO{\cdot}7Al_2O_3$: $Eu^{2+}Dy^{3+}$. The material shows very strong absorption in the UV band from 250 to 390 nm. After excitation, the ceramic will emit visible lights with two different wavelengths, 400 and 486 nm. This kind of two-peak-emission is quite different from the other kinds of long persistent aluminate phosphors. According to literature [11], the other aluminates show only one emitting wavelength, such as 520 nm for $SrO{\cdot}Al_2O_3$:$Eu^{2+}Dy^{3+}$, 500 nm for $BaO{\cdot}Al_2O_3$:$Eu^{2+}Dy^{3+}$ and 440 nm for $CaO{\cdot}Al_2O_3$:$Eu^{2+}Nd^{3+}$. The two peak emission is due to the luminescent nature of Eu^{2+} in $4SrO{\cdot}7Al_2O_3$ ceramic matrix. The Eu^{2+} ions introduced in the lattice are to replace the original Sr^{2+} ions. The novel luminescence of $4SrO{\cdot}7Al_2O_3$: $Eu^{2+}Dy^{3+}$ is determined by the Eu^{2+} site in the $4SrO{\cdot}7Al_2O_3$ lattice. The lattice structure of $4SrO{\cdot}7Al_2O_3$ in the [001] plane is shown in Fig. 4. Both Al^{3+} and Sr^{2+} ions in the lattice have two alternative coordinators, 4 and 6 for Al^{3+} and 6 and 8 for Sr^{2+}, respectively. When Eu^{2+} ions replace Sr^{2+} ions, Eu^{2+} ions will also get two different sites with coordinator of 6 or 8. This means, the crystal environment of Eu1 and Eu2 are quite different. Therefore, when the phosphor is activated by UV light, the surrounding O anions will have different effect on the Eu^{2+} ions, and thus cause two different emissions. Therefore, the different lattice sites, Eu1 and Eu2, are responsible for the emission at 400 and 486 nm, respectively.

3.3. Effect of B_2O_3 on photoluminescent property

Fig. 5 shows the emission curves of $4SrO{\cdot}7Al_{2-x}B_x$:$Eu^{2+}Dy^{3+}$ ceramics with different B_2O_3 content, from $x=0$ to $x=0.2$. It is found by comparison between these curves that, the emission of the luminescent ceramics changes with B_2O_3 content. This change takes

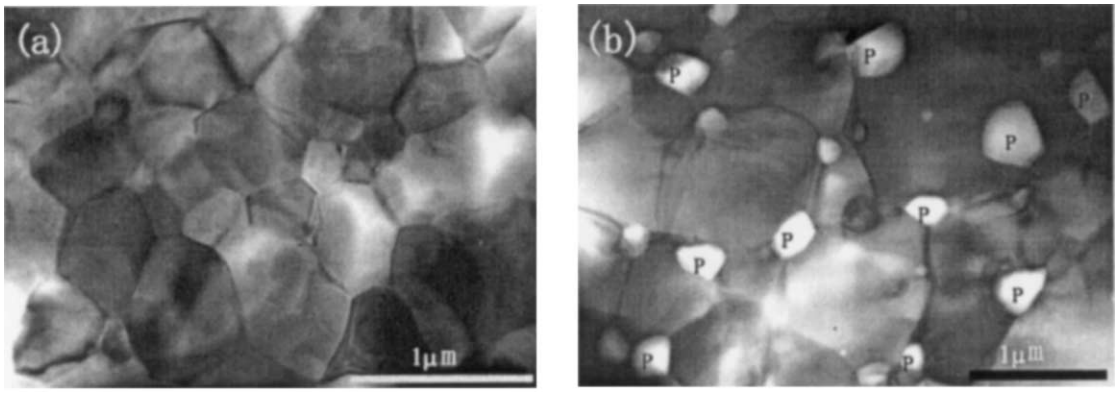

Fig. 2. TEM micrographs of $4SrO{\cdot}7Al_{2-x}B_xO_3$:$Eu^{2+}Dy^{3+}$ ceramics (a) $x=0.2$ and (b) $x=0$.

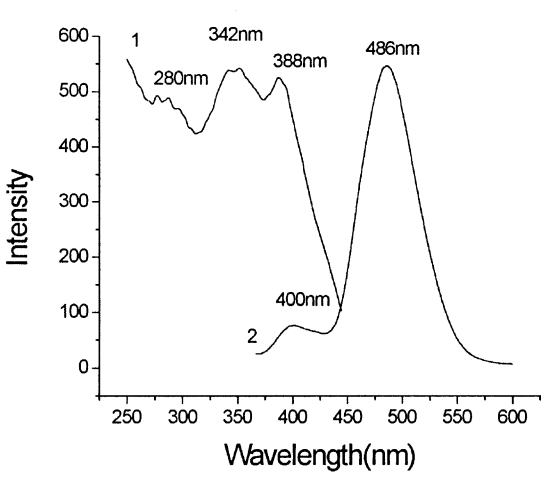

Fig. 3. Excitation and emission spectra of $SrO{\cdot}Al_2O_3$:$Eu^{2+}Dy^{3+}$ ceramics.

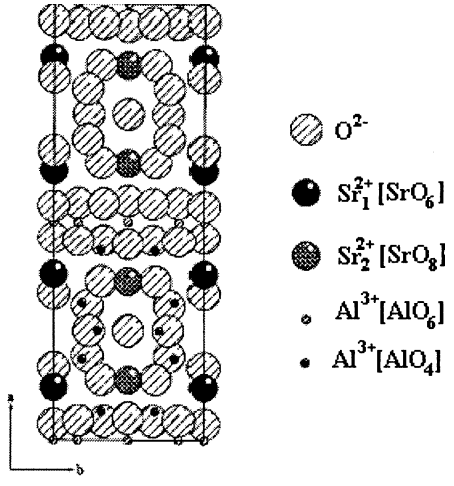

Fig. 4. Projection of the unit cell of $SrO{\cdot}AlO_3$:$Eu^{2+}Dy^{3+}$ along the [001] direction.

place in both the emission intensity and the emission wavelength. Firstly, the intensity of emission at 400 nm increases with the increment in B_2O_3 content, while the intensity of emission at 486 nm almost remains the same. Secondly, both two emission peaks shift to the short wavelength side with the increase in B_2O_3 content. The increase in emission intensity can be ascribed to the different lattice sites that Eu^{2+} pose in the $4SrO{\cdot}7Al_2O_3$ crystal. As discussed above, there are two Sr^{2+} sites that can be replaced by Eu^{2+} ions. These sites held coordinators of 6 and 8, respectively. The size of the two sites are different, site with eight coordinators is much bigger than that with six coordinators. When Eu^{2+} replaces Sr^{2+}, it is easier for Eu^{2+} to pose the site with eight coordinators. That is, Eu^{2+} ions tend to hold the lattice sites with eight coordinators rather than those with six coordinators. Therefore, the concentrations of Eu^{2+} in the two sites are quite different. This difference leads to a weak emission at 400 nm and a strong emission at 486 nm. When B_2O_3 is introduced, it plays the role of flux, helps Eu^{2+} ions squash into the sites with six coordinators. Therefore, with the increment in B_2O_3 content, the concentration of Eu^{2+} ions in six-coordinated sites gradually increases and the related emission is enhanced.

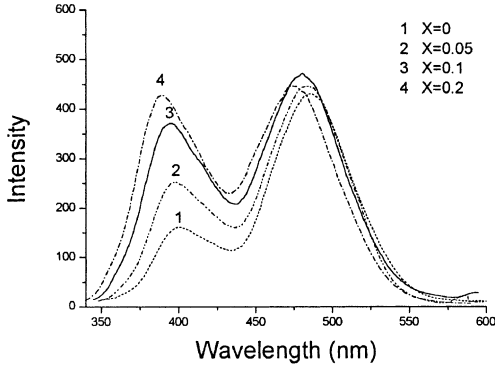

Fig. 5. Emission of $4SrO{\cdot}7Al_{2-x}BO_3{:}Eu^{2+}Dy^{3+}$ with different B_2O_3 content.

The shift in emission peak listed in Table 2 revealed another role of B_2O_3 in the formation of $4SrO{\cdot}7Al_2O_3$ ceramics. Since B^{3+} and Al^{3+} come from the same family of IIIA, and they have the same valence, B^{3+} ions can replace Al^{3+} ions in the four coordinator sites in the synthesis process. The ion radius for B^{3+} in four coordinators is 0.12 Å and that for Al^{3+} is 0.39A. That is, the lattice is contracted when B^{3+} ions replace Al^{3+} ions in the lattice. The lattice parameters calculated by computer software are listed in Table 3, and the contractions in the directions of axes and cell volume are shown in Fig. 6. It can be seen from Fig. 6 that, the contraction mainly take place along *a* and *b* axes, while the contraction in c axes does not happen. It is just the lattice contraction, that reduces the attraction force on Eu^{2+} in the luminescent center and thus cause the blue shifts of the emission peaks.

Table 2
Emission peak shifts for $4SrO{\cdot}7Al_{2-x}B_xO_3{:}Eu^{2+}Dy^{3+}$ with different B_2O_3 content

$4SrO{\cdot}7Al_{2-x}O_3{:}Eu^{2+}Dy^{3+}$	Peak around 400 nm (nm)	Peak around 486 nm (nm)
$x=0$	400	486
$x=0.05$	398	485
$x=0.1$	394	479
$x=0.2$	389	414

Table 3
lattice contraction of $4SrO{\cdot}7Al_{2-x}BO_3{:}Eu^{2+}Dy^{3+}$ ceramics with different B_2O_3 content

$4SrO{\cdot}Al_{2-x}B_xO_3{:}Eu^{2+}Dy^{3+}$	a (Å)	b (Å)	c (Å)	d (Å)
$x=0$	24.7245	8.4854	4.8881	1025.54
$x=0.05$	24.6921	8.4536	4.8865	1019.99
$x=0.1$	24.6008	8.4072	4.8871	1010.77
$x=0.2$	24.5318	8.3759	4.8842	1003.59

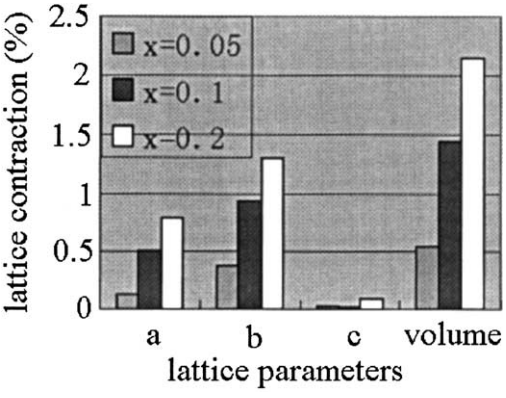

Fig. 6. Lattice contraction of the sintered ceramics.

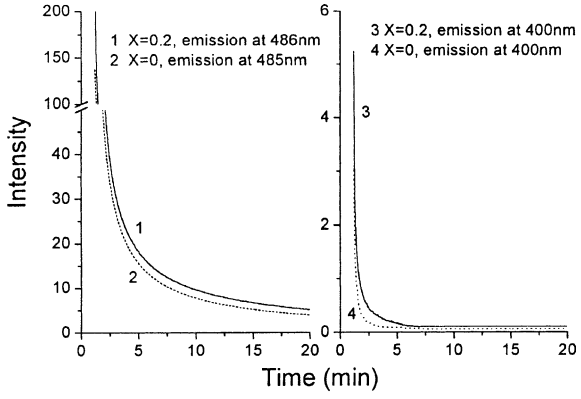

Fig. 7. Afterglow of $4SrO{\cdot}7Al_{2-x}BO_x{:}Eu^{2+}Dy^{3+}$ ceramics.

Table 4
Decay parameters for $4SrO{\cdot}7Al_{2-x}B_xO_3{:}Eu^{2+}Dy^{2+}$ ceramics with $x=0$ and $x=0.2$

B_2O_3 content (mol)	Parameters						
	I_0	A_1	τ_1 (s)	A_2	τ_2(s)	A_3	τ_3(s)
0	5.2252	220.529	0.10309	98.891	0.59704	31.864	4.36062
0.2	3.4361	176.523	0.17329	67.295	0.88785	24.523	5.20001

3.4. Afterglow characteristics of $SrO{\cdot}7Al_{2-x}B_xO_3{:}Eu^{2+}Dy^{3+}$ ceramics

The long persistent behaviors of obtained $SrO{\cdot}Al_{2-x}B_xO_3{:}Eu^{2+}Dy^{3+}$ ceramics, with $x=0$ and $x=0.2$, are shown in Fig. 7. It is clear from the curves that the emission at 400 nm shows very poor duration. The initial intensities after UV activation are low and they only can last for about 5 min. The introduction of B_2O_3 seems to have no significant promotion on the duration. Therefore, the emission around 400 nm is of minor practical importance and is assumed not to contribute to the long persistent characteristics. The main contribution comes from the emission at 486 nm. Both curve 1 and curve 2 show good persistence, and the $SrO{\cdot}7Al_{2-x}B_xO_3{:}Eu^{2+}Dy^{3+}$ ceramics aided by 0.2 mol B_2O_3 (with $x=0.2$) shows a longer afterglow than the ceramics without B_2O_3 addition, indicating that the long persistent property was enhanced by the introduction of B_2O_3.

It is reported that the decay behavior can be fitted by an empirical equation stated as following [12]:

$$I = I_0 + A_1\exp(-t/\tau_1) + A_2\exp(-t/\tau_2) + A_3\exp(-t/\tau_3)$$

where I represents the phosphoresence intensity, I_0, A_1, A_2, A_3 are constants, t is the time, t_1, t_2 and t_3 are the decay times for the sintered ceramics. Using computer software, the decay curves of both the ceramics with and without the addition of B_2O_3 were simulated by the equation to understand the effect of B_2O_3 on the long persistent property. The fitting curves for two ceramics were shown in Fig. 8. Both the decay data for two kinds of ceramics obtained in the experiment fitted the equation very well and the parameters generated from the fitting result were listed in Table 4. According to the literature [12], which report the long lasting mechanism of $CaAl_2O_4{:}Eu^{2+}Dy^{2+}$ $BaAl_2O_4{:}Eu^{2+}Dy^{3+}$ and $SrAl_20_4{:}Eu^{2+}D^{2+}$, the increase in duration was related to the value of τ. The greater the value, the longer the duration. This finding is in good accordance with the results obtained in our experiment and thus was applied in our discussion. The difference in τ_1, τ_2 and τ_3 indicates that there are three kinds of decay process in the phosphorescent ceramics. The largest value, τ_3, can be related to the deepest trap center. The value for τ_3 obtained in the case of 0.2 mol B_2O_3 aided ceramics are

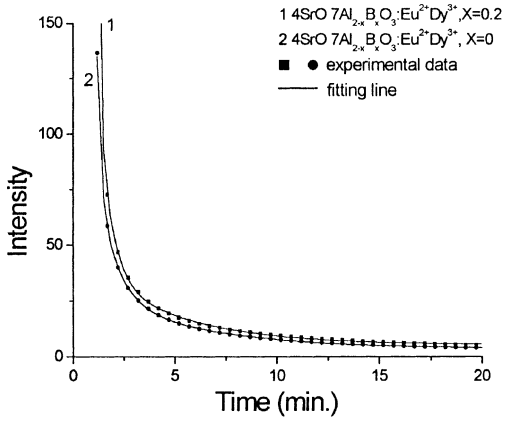

Fig. 8. Simulating of the afterglow curve by the nonlinear least squares fitting.

greater than that of ceramics without B_2O_3 addition, indicating a longer duration was achieved by the help of B_2O_3. Although the introduction of B_2O_3 in the phosphor did not create new trap center in the ceramics, it helped to increase the depth of the trap center and hence led to a slower decay speed than what is observed in the case of the ceramics without B_2O_3. Therefore the afterglow property was enhanced by the introduction of B_2O_3.

4. Conclusion

$4SrO{\cdot}7Al_2O_3$ long persistent ceramics were prepared by sintering method in the experiment. In the sintering process, B_2O_3 stimulated the formation of $4SrO{\cdot}7Al_2O_3$ phosphors and helped to produce dense ceramics at 1400 °C. The ceramics show a two peak emission at 400 and 486 nm, due to the different lattice sites Eu^{2+} ions hold in the $4SrO{\cdot}7Al_2O_3$ lattice. Both the two emission peaks shift to the short wavelength side with the increment in B_2O_3 content due to the lattice contraction caused by the ion replacement between B^{3+} and Al^{3+}. The emission at 400 nm showed very weak afterglow characteristics while the emission at 486 nm illustrated good long persistent property that can be fitted by an empirical equation. The afterglow property was enhanced by the introduction of B_2O_3 due to the increase in the decay time that can be related to the trap center caused by Dy^{3+}.

Acknowledgements

This work was financially supported by Natural Science Foundation of Shanghai (contract no. O2ZE 14055) and Shanghai Nanotechnology Promotion Center (contract no. 0252nm018).

References

[1] B. Rutten Smets, O. J. Hoeks, $2SrO{\cdot}3Al_2O_3{:}Eu^{2+}$ and 1.29 (Ba·Ca)$06Al_2O_3{:}Eu^{2+}$ two new blue emitting phosphors, J. Electrochem. Soc. 136 (7) (1989) 2119–2123.

[2] F.C. Palilla, A.K. Levine, M.R. Tomkus, Fluorescent properties of alkaline earth aluminates of the type MAl_2O_4 activated by europium, J. Electrochem. Soc. 115 (6) (1968) 642–644.

[3] W.Y. Jia, H.B. Yuan, L.Z. Lu, Phosphorescent dynamics in $SrAL_2O_4{:}Eu^{2+}$, Dy^{2+} single crystal fibers, J. Lumin. 76–77 (1998) 424–428.

[4] H. Takasaki, S. Tanabe, T. Hanada, Long lasting afterglow characteristic of Eu, Dy codoped $SrO{\cdot}Al_2O_3$ phosphor, J. Ceram. Soc. Jpn. 104 (4) (1996) 322–326.

[5] Z.L. Tang, F. Zhang, Z.T. Zhang, Luminescent properties of $SrAl_2O_4$: Eu, Dy material prepared by the gel method, J. Eur. Ceram. Soc. 20 (12) (2000) 2129–2132.

[6] T. Katsumata, T. Nabae, K. Sasajima, Growth and characteristics of long persistent $SrAl_2O_4$ and $CaAl_2O_4$ based phosphor crystals by a floating zone technique, J. Cryst. Growth 183 (3) (1998) 361–365.

[7] H. Yamamoto, T. Matsuzawa, Mechanism of long phosphorescence of $SrAL_2O_4{:}\ Eu^{2+}$, Dy^{3+} and $CaAl_2O_4{:}\ Eu^{2+}$, Nd^{3+}, J. Lumin. 72–74 (1997) 287–289.

[8] Y.H. Lin, Z.L. Tang, Z.T. Zhang, Preparation of long-afterglow $Sr_4Al_{14}O_{25}$-based luminescent material and its optical properties, Mater. Lett. 51 (1) (2001) 14–18.

[9] M. Akiyama, C. Xu, H. Matsui, Photostimulated luminescence phenomenon of $Sr_4Al_{14}O_{25}$: Eu, Dy using only visible lights, J. Mater. Sci. Lett. 19 (13) (2000) 1163–1165.

[10] D. Wang, M.Q. Wang, G.L. Lu, Synthesis, crystal structure and X-ray powder diffraction data of the phosphor matrix $4SrO{\cdot}7Al_2O_3$, J. Mater. Sci. 34 (20) (1999) 4959–4964.

[11] T. Katsumata, R. Sakai, S. Komuro, Growth characteristics of long duration phosphor crystals, J. Cryst. Growth 199 (1999) 869–871.

[12] Y.H. Lin, Z.T. Zhang, Z.L. Tang, The characterization and mechanism of long afterglow in alkaline earth aluminates phosphors co-doped by Eu_2O_3 and Dy_2O_3, Mater. Chem. Phys. 70 (2) (2001) 156–159.